

Adsorption of a basic dye, Methylene Blue, in aqueous solution on bentonite

H. AIT HMEID^{(a)*}, M. AKODAD^(a), M. BAGHOUR^(a), A. MOUMEN^(a), A. SKALLI^(a), G. AZIZI^(a), A. ANJJAR^(b), M. AALAOUL^(c), L. DAOUDI^(d)

^(a) Laboratory Observatory of the Marchica Lagoon of Nador and Limiting Regions (OLMAN-RL), Multidisciplinary Faculty of Nador, Mohamed 1st University, 60700 Nador –Morocco.

^(b) Laboratory of Georessources and environment (GRE), Faculty of Science and Technology, University Sidi Mohamed Ben Abdellah, B.P.2202- Imouzzer Road, Fes, Morocco.

^(c) Laboratory of Applied Geosciences, Faculty of Sciences of Oujda, Mohamed 1st University, 60000 Oujda-Morocco.

^(d) Laboratory of Geosciences Georesources s and Environment, Department of Geology, Faculty of Science and Technology University Cadi Ayyad, Marrakech –Morocco.

Abstract

The dyes are used in many industrial sectors such as textiles, paper and leather dyeing, as well as in the food and cosmetics industry. Dyes are known to be toxic and persistent in the environment and require physico-chemical techniques to degrade them. This work deals with the study of the adsorption of the cationic dye methylene blue on raw bentonite from the region of Nador (Morocco). The physico-chemical properties show that our bentonite indicates a very high alkalinity. The amplitude of swelling shows that this bentonite is very high is sensitive to water. The SEM shows petaloid-shaped aggregates of the grains in spherical form with heterogeneous dimensions. Various experimental parameters were analyzed; initial concentration of the dye, pH, mass of the adsorbent and temperature. Adsorption tests showed that the maximum duration of this cationic dye on bentonite is established after 80 minutes. Experimental results showed that the adsorption of the methylene blue dye on raw bentonite depends on the pH of the solution and the initial concentration of the dye. Although the amount of methylene blue adsorbed decreases with increasing temperature, this indicates that adsorption is an exothermic process. The adsorption capacity was determined using the Langmuir, Freundlich, Elovich and Temkin isotherms. The binding of methylene blue follows Freundlich's law.

* Corresponding author:

hanane.aithmeid@gmail.com

Received 23 Oct 2020,

Revised 03 Oct 2021,

Accepted 05 Oct 2021

Keywords: bentonite, adsorption, Morocco, SEM, heterogeneous, Freundlich, methylene blue.

1. Introduction

The industrial activities are a very important source of pollution and contribute in a certain way to the deterioration of the environment [1, 2, 3]. The discharges of effluents from the textile industries, in particular the various dyes which are used in excess in dyeing of paper, cotton, wool and silk [4, 5, 6]. As a result, the waste water is highly concentrated in colorant. Most of the dyes are toxic and carcinogenic compounds, which have a detrimental effect on public health and can greatly harm animal and plant species as well as the various microorganisms living in these waters [7, 8, 9, 10]. Although causing breathing difficulties, nausea, vomiting, tissue necrosis, profuse sweating, the mental confusion, cyanosis and methemoglobinemia [11]. Different conventional methods have been used to remove pollutants from water, the most usable methods are done by chemical-physicochemical or biological means including coagulation/flocculation [12, 13, 14]. Which is a process that removes suspended particles, precipitation and membrane filtration and adsorption, which is the most effective and widely used treatment process [15]. Thus to remove the dyes there are several adsorbents, the most well known is activated carbon (with activation) [16, 17, 18], diatomite, chitosan, pyrophyllite [19], eucalyptus-based biomaterials [20, 21], biosorbent at the base of date nuclei [22], clay [23, 24], zeolite [25, 26], and Cellulose-Ether Based adsorbent [27]. After the characterization of bentonite, we will evaluate the impact of the adsorption capacity to remove a cationic dye called Methylene Blue (MB). During this study, we varied several kinetic parameters such as concentration, pH, reaction temperature, contact time and adsorbent mass. The experimental results were analyzed to study the equilibrium and thermodynamic aspect of the methylene blue adsorption process on raw bentonite without activation.

2. Materials and experimental procedures

2.1. Materials

The bentonite used in this study was collected from the Trebia deposit, located on the northwestern flank of the Tidiennit massif in the Nador region which belongs to the outer domain of the Moroccan Rif chain (figure 1) [28]. It was dried in an oven at 48°C for 24 h, before experiments. The basic dye, Methylene Blue (MB), was used as an adsorbate to determine the efficacy of crude bentonite with a 500 mg.L⁻¹ (table 1).

Table 1. Properties and characteristics of MB

Generic name	Methylene blue
Generic Nomenclature	Basic Blue 9
Index color	52015
Melting temperature	180°C
Chemical Formula	C ₁₆ H ₁₈ C ₁ N ₃ S·3H ₂ O
Molar weight (g/mol)	319,85
Molecular volume (cm ³ /mol)	241.9
Wave length (λ_{max})	665 nm

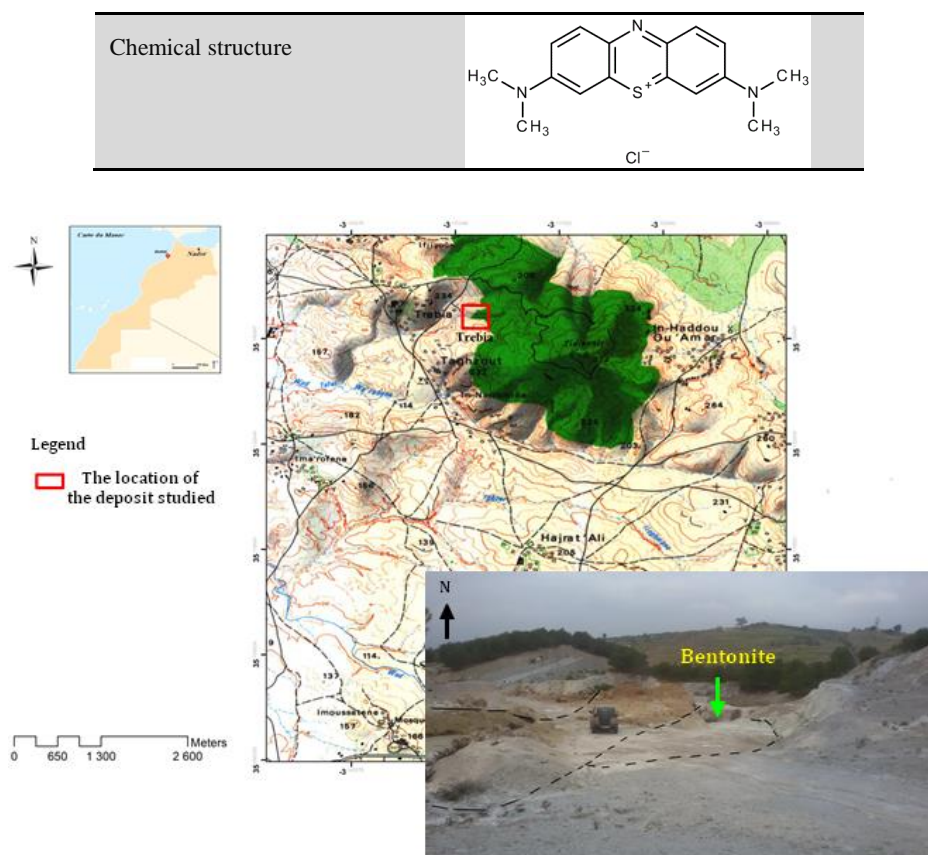


Figure 1. The location of the bentonite sample used.

2.2. Experimental procedures

2.2.1. Characterization of the adsorbent

The surface morphology has been carried out using scanning electron microscopy (SEM). The particle size distribution of bentonite powder was determined by using laser diffraction particle size analyzer Horiba 300. The mineralogy of sample was evaluated using X-ray diffraction technique and was performed on an Burker D8 diffractometer operating at a voltage of 40 kV and an intensity of 30 mA with radiation (Cu), on the powdered sediments following the normal procedure for clay analysis [29]. Fourier transform infrared spectroscopy (FTIR) provides valuable information on absorbed water molecules and structural hydroxyl groups of clay minerals [30]. In this study, the Casagrande apparatus was used to determine the liquidity limit using the method described by Casagrande (1947) and Andrade et al, (2011) [31, 32]. The values of the total specific surface area (Sst) and cation exchange capacity (CEC) were derived from the methylene blue test [33, 34, 35]. The swelling index was performed on 2 g of bentonite powder added to distilled water. After 24–48 h, the swelling volume was measured according to the methodology described by Qlihaa et al. (2016) [36].

2.2. 2. Study of kinetic parameters

In order to determine the equilibrium concentration of the adsorbate. However, the experimental solutions of the desired initial concentrations were obtained by diluting the MB stock solution (500 mg.L⁻¹). Indeed, we varied the concentrations from 5 to 500 mg.L⁻¹. In order to evaluate the effect of the initial pH on the adsorption efficiency and to determine the optimal pH of the adsorption, the adsorption of methylene blue on bentonite was performed at pH values ranging from 2 to 10. In order to study the effect of temperature, we follow the adsorption of Methylene Blue at

different temperatures ranging from 20°C to 100°C. The study of the influence of the contact time on the rate of fixation of our dye on the bentonite allowed us to determine the equilibrium time corresponding to a state of saturation of the adsorbate by the adsorbent. We follow the adsorption of Methylene Blue at time intervals from 0 to 100 min. We show the evolution of the fixation rate of our cationic adsorbate (MB) as a function of the mass of the adsorbent (bentonite). A series of experiments was carried out to determine the optimal mass of the adsorbent. The adsorption of methylene blue on bentonite was carried out at various masses from 0.1 to 0.4g. After equilibrating the suspensions, the adsorption of the aqueous solution of Methylene Blue of all parameters was determined by UV-vis spectrophotometry type Shimadzu. The experiment parameters are shown in Table 2. The removal efficiency (R) and equilibrium adsorption capacities (qe) and are calculated according to equations (1) and (2) as follows:

$$R = \frac{C_0 - C_e}{C_0} \times 100 \quad (1)$$

$$qe = \frac{(C_0 - C_e)V}{m} \quad (2)$$

Where C_0 and C_e are the initial and equilibrium concentrations of MB (mg.L^{-1}); qe and R are the uptake amount (mg.g^{-1}) and the removal rate (%) at equilibrium respectively; V is the volume of the solution (L); and m is the mass of the adsorbent (g).

Table 1. Experimental design for batch adsorption study

Investigation	Control parameters	Variable parameters
Effect of concentration	Initial concentration: 500 mg.L^{-1} The mass of adsorbent: 0,3 mg	Solution concentration (mg.L^{-1}): 5, 10, 15, 20, 30, 50, 100, 150, 200, 250, 300, 350, 400, 450, 500.
Effect of pH	Initial concentration: 20 mg.L^{-1}	Solution pH 2, 3, 4, 5, 6, 7, 8, 9, 10
Effect of temperature	The mass of adsorbent: 0,3g Initial concentration: 20 mg.L^{-1}	Solution temperature ($^{\circ}\text{K}$): 20, 30, 40, 50, 60, 70, 80, 90, 100.
Effect of mass	Initial concentration: 20 mg.L^{-1} Volume : 10ml Temperature 25 $^{\circ}\text{K}$ Contact time = 60 min	The mass of adsorbent (g): 0.1, 0.15, 0.2, 0.25, 0.3, 0.35, 0.4
Adsorption kinetics	The mass of adsorbent: 0,3g Initial concentration: 20 mg.L^{-1}	Contact time (min): 0, 10, 20, 40, 60, 80 à 120

2. 2. 3. Isothermes d'adsorption

Adsorption isotherms are used for the determination of capacities pollutant fixation and the identification and understanding of the maximum pollutant fixation adsorption mechanisms. For the study of adsorption isotherms applied to describe the adsorption process our experimental results are: Langmuir, Freundlich, Elovich and Temkin

isotherms. The Langmuir isotherm is one of the models describing monolayer adsorption. The linear form of the Langmuir isotherm can be expressed by the following equation (3) [37, 38]:

$$\frac{q_e}{q_m} = \frac{k_L \cdot C_e}{(1 + K_L \cdot C_e)} \quad (3)$$

Where q_e (mg.g⁻¹): the quantity adsorbed at equilibrium; C_e (mg.L⁻¹): the concentration at equilibrium; q_m (mg.g⁻¹): the maximum quantity adsorbed; K_L (L.mg⁻¹): Langmuir's constant.

The Freundlich model is an empirical equation used to describe the systems heterogeneous. Freundlich's linear equation is represented by the following equation (4) [39]:

$$q = k_f \cdot C_e^{1/n} \quad (4)$$

Where K_f (mg.g⁻¹): the Freundlich constant which expresses the adsorption affinity; $1/n$: the Freundlich constant related to the binding energy; n : the heterogeneity factor;

The Elovich isotherm is dependent on the kinetic development, assuming that the adsorption sites increase exponentially with adsorption [40]. This implies a multilayer adsorption. The Elovich isotherm is described by equation (5):

$$\ln \frac{q_e}{C_e} = \frac{q_e}{q_m} + \ln(K_e q_m) \quad (5)$$

Where, K_e (L.mg⁻¹): the equilibrium constant of Elovich; q_m (mg.g⁻¹): the maximum capacity of Elovich;

The derivation of the Temkin isotherm assumes that the decrease in the heat of adsorption is linear rather than logarithmic, as applied in the Freundlich equation. The Temkin isotherm has generally been presented by the following equation (6):

$$q_e = \frac{RT}{b} \ln K_T + \frac{RT}{b} \ln C_e \quad (6)$$

Where, q_e (mg.g⁻¹): the quantity of metal ions adsorbed; C_e (mg.L⁻¹): the equilibrium concentration of the solute; R (kJ.mol⁻¹): the universal gas constant; T (°K): the temperature; b : the constant dependent on the adsorption energy; K_T (L / mg): the equilibrium constant;

3. Results and discussion

3.1. Characterization of adsorbent

3.1.1 Physicochemical and geotechnical properties

Tables 3 exhibit the results of the physicochemical and geotechnical properties of the raw bentonite used such as adsorbent. Raw bentonite of Nador is characterized by the clay fraction (< 2µm) in the order of 3.724 %, the silt fraction from 41.63 % and the sand fraction from 54.63% [41]. The surface of Trbia's bentonites is about 271.81 m².g⁻¹. The high CEC value indicates that the bentonite used in this study is rich in montmorillonites. The water content is quite high, of the order of 30.7%. This value of the natural water content can be related to the amount of fine elements or clay contained in the analyzed sample [42]. Although it indicates a very high alkalinity, which would be due to soluble and basic salts such as alkali carbonates and bicarbonates or silicates [43]. These soluble and basic salts are generally part of the composition of the clay [44, 36]. The geotechnical tests that are covered in this study are those that can be used to evaluate the probable performance of the raw bentonite, either by swelling tests or by Atterberg limits give concordant results. These are very plastic bentonites, have a very high swelling potential. These results show that the bentonite are inactive, the A_{CB} value from 3.48 [35].

Table 3. Results of physico-chemical and geotechnical properties of bentonite.

<i>Properties</i>		
Physico-chemical	Percentage sand (> 60 μm)	54.63
	Percentage silts (2–60 μm)	41.63
	Percentage clay (<2 μm)	3.72
	Sst (m^2/g)	271.81
	CEC (meq/100g)	30.5
	pH	8.43
Geotechnical	A_{CB}	3.48
	IG (%)	72.5
	LL (%)	102
	PL (%)	42
	PI (%)	60
	Water content (W %)	30.7

Note: * S_{st} , specific surface area ; CEC , Cation exchange capacity ; A_{CB} , clay activity ; IG , swelling index ; LL , Liquidity limit; PL , plasticity limit; PI , plasticity index.

3. 1.2 Characterization by X-ray diffraction

The total mineralogical composition of the raw bentonite studied is very diverse (Figure 2). X-Ray Diffractograms (XRD), analysis of raw bentonite shows the presence of montmorillonite as the major component. Dolomite, zeolite, feldspar, anatase, xenotime, pyrite, hematite, anorthite, cristobalite, and quartz are also present.

The XRD diffractogram is characterized by two types of montmorillonites. Of which, the diffraction peak (001) of the montmorillonite appears at a basal spacing of 15 Å corresponds to a calcium (M-Ca) pole and the diffraction peak (001) appears at a basal spacing of 12 Å corresponds to a sodium (M-Na) pole [45, 46]. The other three peaks are located at 4.48 Å (d_{110}), 2.16 Å (d_{200}) and 1.49 Å (d_{060}). The reflection d_{060} at 1.49 Å indicates the dioctahedral character of smectite [45, 47].

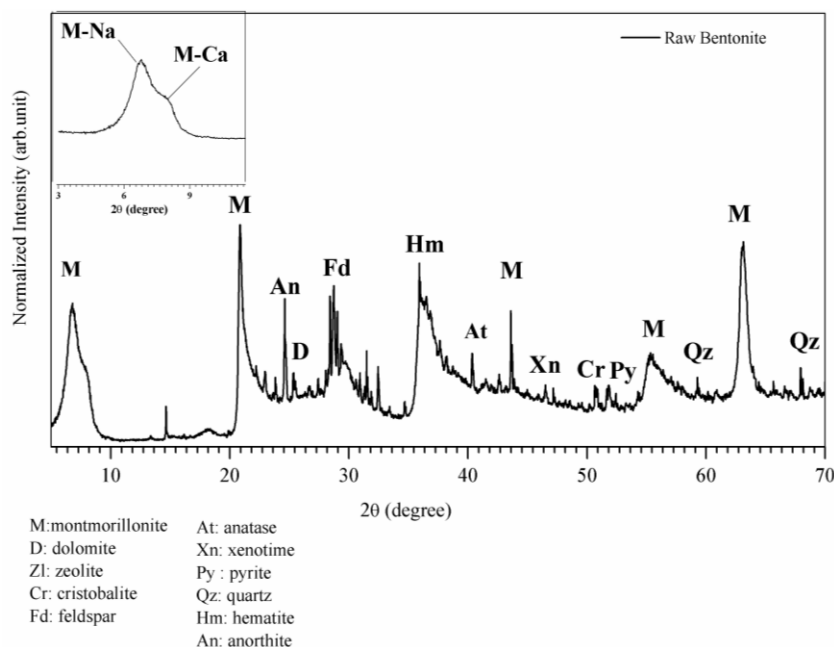


Figure 2. X-ray diffractogram of raw Moroccan bentonite.

3.1.3 FTIR Spectrum Analysis

The FTIR analysis of the raw bentonite was taken in the range of 400–4000 cm^{-1} . The FTIR spectra of both are shown in Figure 3. The spectrum of the raw bentonite exhibits a very strong multiple absorption band observed from 3699.47 to 3251.98 cm^{-1} , these bands are attributed to the bond elongation vibrations of the hydroxylated [O-H] groups in the montmorillonite structure at the octahedral layer coordinated with two aluminum atoms [48]. The 3251.98 cm^{-1} band attributed to the OH stretching (ν_3) of the structural hydroxyl groups and water present in the mineral indicates the possibility of a hydroxyl bond between the octahedral and tetrahedral layers [49]. However, a very strong and intense band was observed at 1643.35 cm^{-1} due essentially to the asymmetric OH elongation (ν_2) that means the OH deformation of the water adsorbed between the layers and the OH elongation of constitution. The vibrations observed at 1035.77 cm^{-1} correspond to the Si-O elongation [46]. The band corresponding to the Al-Al-OH deformation is observed at 914.26 cm^{-1} [50, 48]. The presence of an 844.82 cm^{-1} band in all band samples is attributed to the Al-Mg-OH deformation. [51]. As well as Al-O-Si, Si-O-Mg and Si-O-Si deformation of clay minerals at 462.92 cm^{-1} [51, 48].

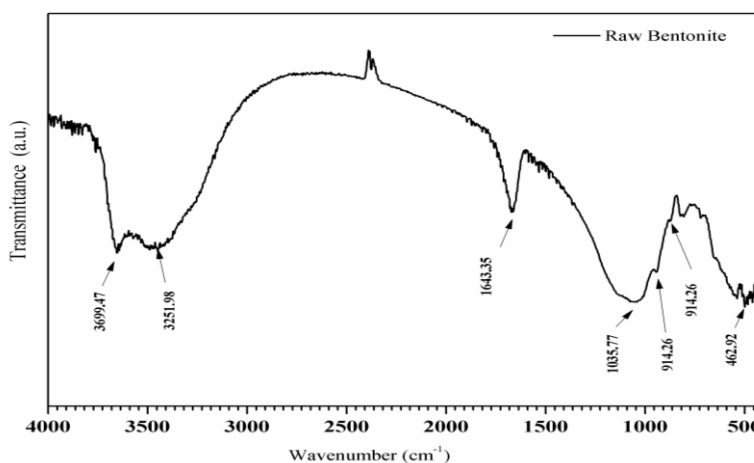


Figure 3. FTIR spectra of raw Moroccan bentonite.

3.1.4 XRF characterization

It was performed to know the chemical compositions of the minerals that are present in the clay. The results exhibit in the table 4 shows that the magnesium, the alumina, calcium, and iron are present with major quantities. However, other minerals are present in trace amounts such as silica, potassium, phosphorus etc. This confirms the mineralogical analysis of bentonite.

Table 4. Chemical analysis raw Moroccan bentonite.

Chemical composition	Weight (%)
Mg	29.28
Fe	28.65
K	4.45
Ca	11.1
Si	0.11
Al	7.29
P	3.11
S	1.593
Ti	1.246
Mn	0.861
Rb	0.0502
Sr	0.376
Zr	0.32
Th	0.106
Zn	0.081
Y	0.02
As	0.012
Sn	0.066

3.1.5 Scanning Electron microscopy

The images obtained by scanning electron microscopy of raw Trebia bentonite with different magnification are shown in the figures below. The SEM image shows petaloid-shaped aggregates of the grains in spherical form with heterogeneous dimensions (Figure 4). See that from the typical shape for smectites [52]. The texture includes a mixture of clay and non-clay minerals, which allows for a heterogeneous environment. The analysis of SEM images reveals the presence of feldspar, zircon, calcic albite, iron oxides, and barite. Thus, this confirms what we have obtained in DRX. With a higher magnification (50 μ m), we observe irregularly shaped pores and fissures. A semi-quantitative EDX analysis of the raw bentonite samples shows the presence of the following elements: Al, Si, Mg, Na, O, K, Fe, Zr, Ba, and Ca. These results confirm those found by chemical analysis which also proved the presence of these elements in the form of oxides: Al, Si, Fe, Mg, Na, Ca and K.

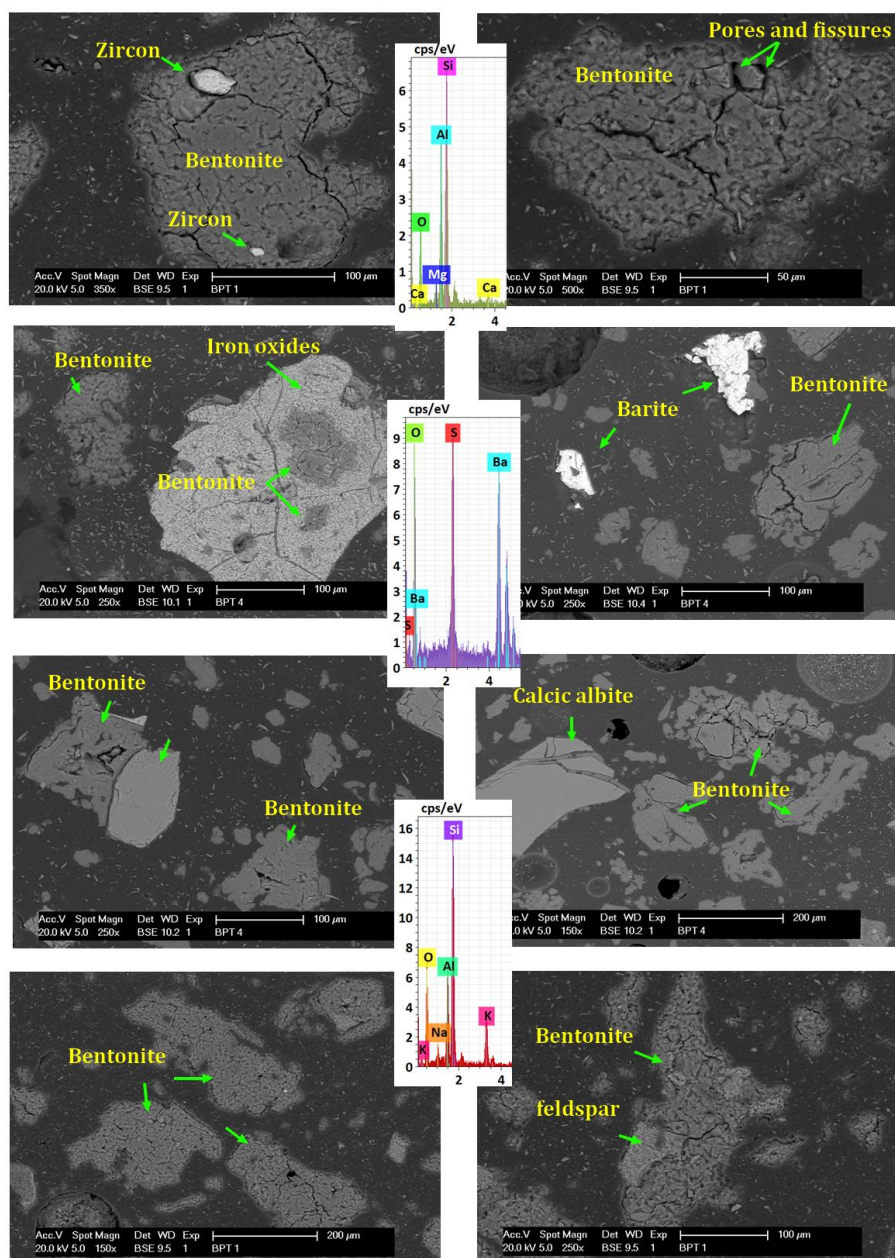


Figure 4. SEM images and EDX spectra of raw bentonite.

3.2. Adsorption studies

3.2.1. Effect of initial concentration

The initial concentration of the dyes is a crucial parameter on the adsorption rate [53, 54]. As shown in Figure 5, we can see that the adsorption capacity increases progressively with the increase of the initial MB content. The quantity of MB adsorbed on raw bentonite increased from 0.33 to 16.66 mg. g⁻¹. The initial concentration of the dye is directly related to the free sites on the surface of adsorbent, in other words, the increase in concentration accelerates the diffusion of the adsorbate to the active surface under the action of the concentration gradient force, therefore one can conclude that the adsorption performance depends on the number of vacant sites on the bentonite surface. Our results similar to the one to be found by Khelifi et al (2016) [55], for the adsorption of methylene blue on a biosorbent based on date nuclei, also a natural biodegradable adsorbent based on Lebanese Eucalyptus [20].

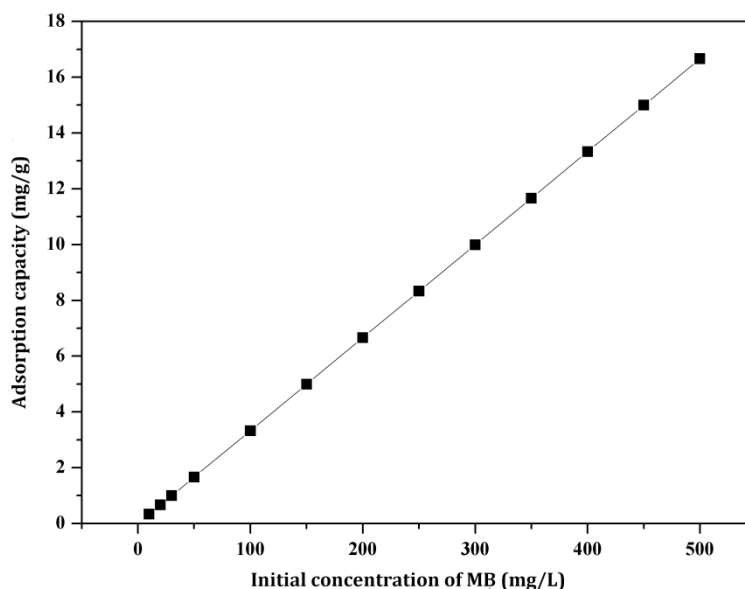


Figure 5. Effect of the initial MB concentration on the adsorption capacity of bentonite ($V = 10\text{ml}$; $m = 0.3\text{g}$; $T = 25^\circ\text{K}$).

3. 2.2. Effect of contact time

The effect of contact time on the MB removal rate was studied for a period ranging from 0 to 100 minutes, with an initial concentration of 20 mg.L^{-1} and at a temperature of 25°C . Determination of the contact time which corresponds to the adsorption/desorption equilibrium or a saturation equilibrium state. The results presented in figure 6 show that the adsorbed quantity of MB increases rapidly in the first 15 minutes to reach an adsorption capacity of about 5mg.g^{-1} and remains approximately constant after 20 minutes, indicating a state of equilibrium. The maximum duration of this cationic dye on bentonite is 80 min. Indeed, from an economic point of view, the fast kinetics ensure a high yield for industries.

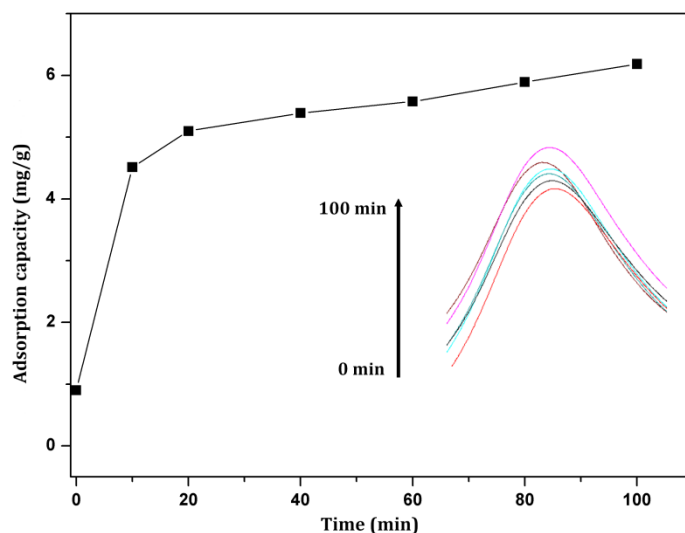


Figure 6. Effect of MB contact time on Bentonite ($C_i = 20\text{mg.L}^{-1}$; $V = 10\text{ml}$; $m = 0.3\text{g}$; $T = 25^\circ\text{K}$)

3. 2.3 Effect of temperature

Temperature is an important physical parameter that can change the adsorption capacity of the adsorbent [56]. The effect of temperature on the adsorption of MB on bentonite was studied in the temperature range of 20 to 100°C under stirring for 30 min. Figure 7 shows the variation of the adsorption capacity as a function of temperature. It can be seen

that the adsorbed quantity of MB decreases with increasing temperature, which indicates that adsorption is an exothermic process. This may be due to the weakening of the attractive forces between the dye species (MB) and the active sites on the adsorbent surface. Indeed the adsorption of MB on bentonite is favorable at low temperatures.

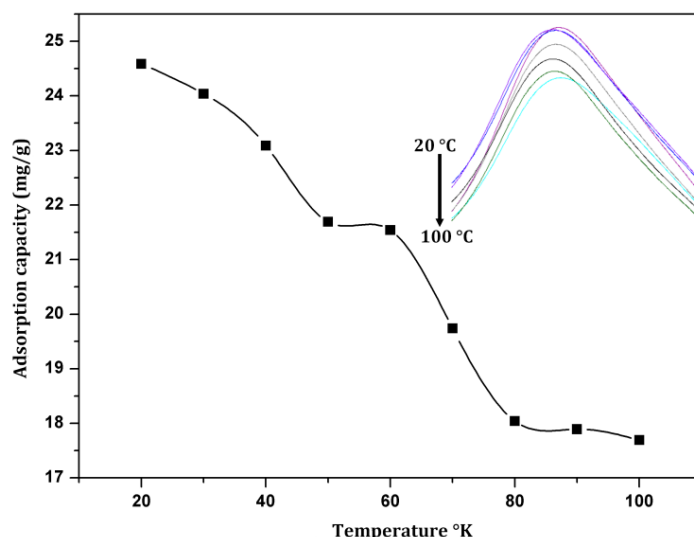


Figure 7. Influence of temperature on the adsorption of MB by bentonite ($C_i=20\text{mg.L}^{-1}$; $V=10\text{ml}$; $m=0.3\text{g}$).

3.2.4 Effects of the adsorbent mass

To determine the optimal mass needed to remove MB, 10ml of the MB 50 mg L^{-1} solution is brought into contact with different masses of crude Trebia bentonite, ranging from 0.1 to 0.4g, under constant stirring for 60 min, and at room temperature. The results presented in figure 8 show an increase in the percentage of adsorption with the mass of the Bentonite. A rapid increase can be inferred when the Bentonite mass is increased from 0.2 to 0.25g. Above 0.30g no variation is observed as the percentage of removal remains almost constant. Indeed the increase in the percentage of adsorption observed as a function of the mass of the Bentonite is due to the availability of free adsorption sites which increases with the quantity of adsorbent up to the mass 0.25g. Our results are similar to the one to be found by Boumchita et al (2016) [57], for the adsorption of methylene blue on potato peelings. As well as the adsorption of MB on *Cucumeropsis mannii* teguments [58]. Therefore, the ideal mass required for MB adsorption is of the order of 0.30g/10ml.

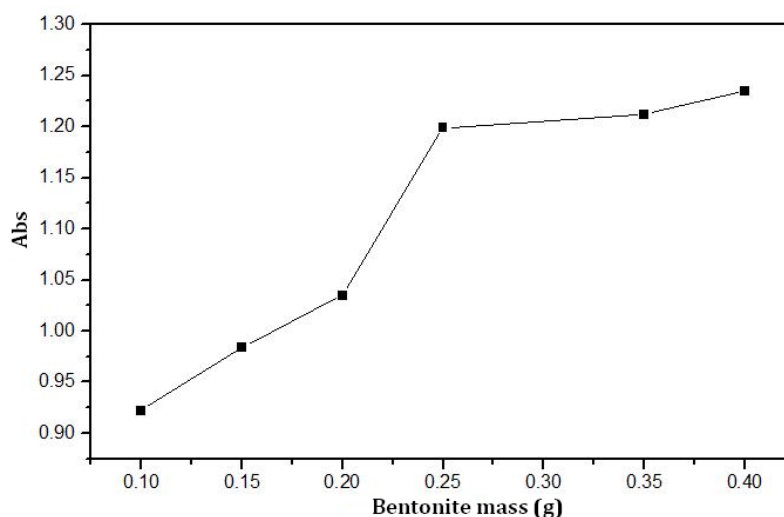


Figure 8. Mass Effect of Bentonite on MB removal ($C_i=20\text{mg.L}^{-1}$; $V=10\text{ml}$; $T=25^\circ\text{K}$; $t_c=60\text{ min}$).

3.2.5 Effect of pH

The pH is an important factor in any adsorption study because it can influence both the adsorbent and adsorbate structure as well as the adsorption mechanism. Indeed, it acts both on the surface charge of the material and on the distribution and speciation of cations [59, 60]. Figure 9 shows a decrease in the adsorbed amount of MB between pH=3-9 from 60 mg.g⁻¹ to a minimum at 46 mg.g⁻¹. It can be seen that the high levels of MB adsorption occur at very low pH values (pH=2), although at basic pH values (pH=11). Thus, in the interval where pH is low, this can be explained by the number of negatively charged sites decreasing and the number of positively charged sites increasing [61, 62, 63]. However, the surface of the adsorbent would be surrounded by H⁺ ions, which decreases the interaction of the ions of the MB (cationic pollutant) with the sites of the adsorbent (bentonite) and prevents the formation of bonds between the MB and the active site [64, 65]. On the other hand, at high pH values, the H⁺ concentration decreases, which leads to a good interaction between the dye ions and the sites on the bentonite surface. In addition the substitution of the cation Ca²⁺ by the cation Na⁺. This process improves the quality of the bentonite, it becomes very swelling and absorbent [45]. A similar observation was previously reported for the adsorption of MB on activated Algerian bentonites [66].

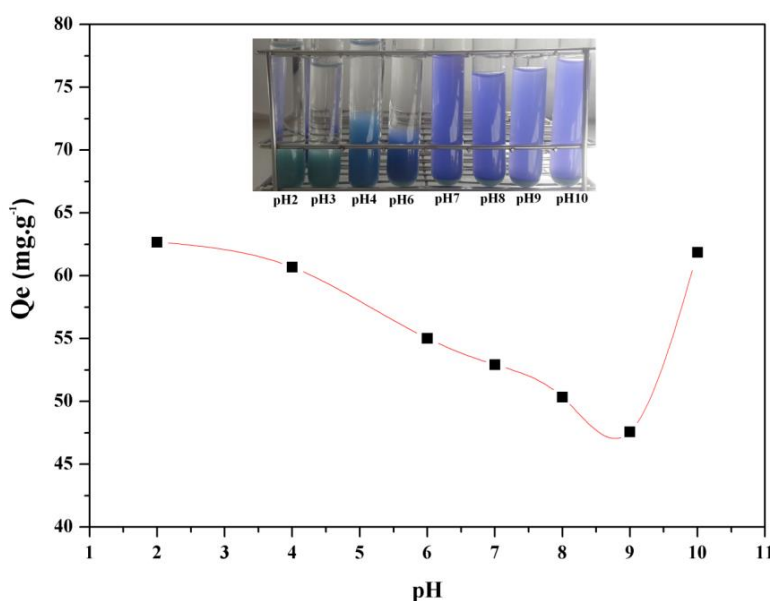


Figure 9. Effect of pH on MB adsorption by bentonite ($C_i=20\text{mg.L}^{-1}$; $V=10\text{ml}$; $m=0.3\text{g}$. $T=25^\circ\text{K}$; $t_c=60\text{ min}$).

3.3. MB adsorption mechanism on bentonite

The adsorption process results from interactions between the surface of the adsorbent (bentonite) and the adsorbate (MB). However, we found that bentonite is characterized by a variety of metal ions such as (Table 4): Al³⁺, Ti³⁺, Zn²⁺, etc., which serve the cation exchange mechanism. As well as the bands attributed to the bond elongation vibrations of the hydroxyl groups [O-H] (figure 3), which are responsible for the appearance of the surface complexation mechanism. Therefore, that the adsorption process of MB on bentonite is carried out according to the ion exchange and surface complexation mechanisms.

3.4. Modelling of MB adsorption isotherms on raw bentonite

The MB adsorption isotherms on bentonite; (a) Langmuir, (b) Freundlich, (d) Elovich and (c) Temkin, are presented in figure 10. Applying the Langmuir isotherm for the bentonite adsorbent, a linear variation with a correlation coefficient of -0.7137 is found. The application of the Freundlich isotherm for the same adsorbent gives a linear correlation

coefficient equal to 0.9747. Elovich isotherm with coefficients of determination (r_{E2}) of the order of 0.85499 and Temkin with a linear correlation coefficient value of the order of 0.9722. The comparison between the linear correlation coefficients (r^2) shows that the adsorption of MB on bentonite, the correlation coefficient in the Freundlich model (r_{F2}) with a value of $=0.9747$, is the highest compared to the other isotherms. Indeed, the adsorption of BM on bentonite is described by the Freundlich isotherm, which means that the adsorption sites present on the surface are energetically heterogeneous, as well as the adsorption is multilayered.

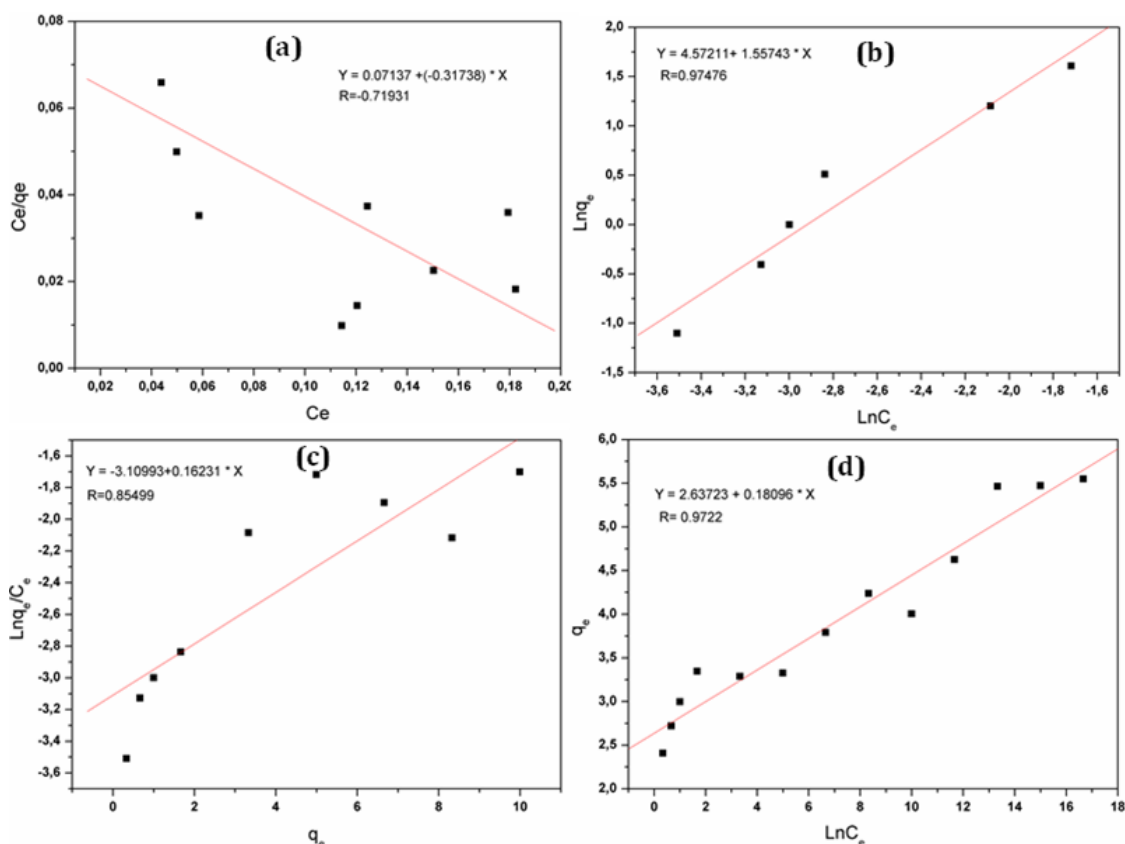


Figure 10. Comparison of MB adsorption isothermal models on bentonite; (a) Langmuir, (b) Freundlich, (c) Elovich and (d) Temkin.

4. Conclusion

The bentonite used in this work was collected in the region of Nador-Morocco. Taking into account all the results of the characterization, it is deduced that Moroccan bentonite has been accepted as an adsorbent. As the mineralogical characterization indicates the dominance of calcium bentonites, this is confirmed by chemical analyses showing that it is calcium bentonites that have high calcium contents. Indeed, this bentonite has a very high water retention capacity, although it is very plastic. They are composed of fine-grained particles that favor their very large specific surface area. Also, the high values of the cation exchange capacity allow us to conclude that our bentonites are rich in montmorillonites, which translates into a better adsorption capacity. This study allows us to optimize the adsorption conditions. The equilibrium data are best described by the Freundlich isotherm. Of which, adsorption evaluation has shown that the removal of MB is exothermic. We conclude that raw bentonite was successfully applied to remove the methyl blue dye in aqueous solution by adsorption. In view of the very encouraging results obtained indicating the potential of these low-cost adsorbent materials for water treatment.

References

- [1] O. KHELIFI., Etude de l'adsorption du nickel et du cuivre sur un charbon actif préparé à partir des boues de station d'épuration. Thèse de doctorat. Université 8 Mai 1945 Guelma, Alger, (2018) 149.
- [2] D. I. Stern, M. S. Common, and E. B. Barbier., Economic growth and environmental degradation: The environmental Kuznets curve and sustainable development, *World Dev.*, 24/7(1996), 1151–1160.
- [3] A. El karkouri, K. Harboul, H. Arroud, and M. El Hassouni, Hexavalent chromium removal from a tannery effluent by a bacterial consortium, *Moroccan Journal of Chemistry*, 7/4(2019), 7-4. <https://doi.org/10.48317/IMIST.PRSM/morjchem-v7i4.17621>.
- [4] M. Rafatullah, O. Sulaiman, R. Hashim, A. Ahmad, Adsorption of methylene blue on low-cost adsorbents : A review, *J. Hazard. Mater.*, 177/1–3(2010) 70–80. <https://doi.org/10.1016/j.jhazmat.2009.12.047>.
- [5] M. M. Hamed, I. M. Ahmed, S. S. Metwally, Adsorptive removal of methylene blue as organic pollutant by marble dust as eco-friendly sorbent, *J. Ind. Eng. Chem.*, 20/4(2014) 2370–2377. <https://doi.org/10.1016/j.jiec.2013.10.015>.
- [6] J. Yan, G. Lan, H. Qiu, C. Chen, Y. Liu, Adsorption of heavy metals and methylene blue from aqueous solution with citric acid modified peach stone, *Sep. Sci. Technol.*, 53/11(2018) 1–11., <https://doi.org/10.1080/01496395.2018.1439064>.
- [7] T. Robinson, G. McMullan, R. Marchant, P. Nigam, Remediation of dyes in textile effluent: a critical review on current treatment technologies with a proposed alternative, *Bioresour. Technol.*, 77/ 3(2001) 247–255. [https://doi.org/10.1016/S0960-8524\(00\)00080-8](https://doi.org/10.1016/S0960-8524(00)00080-8).
- [8] T. Akar, S. Tunali, Biosorption characteristics of *Aspergillus flavus* biomass for removal of Pb(II) and Cu(II) ions from an aqueous solution, *Bioresour. Technol.*, 97/15(2006) 1780–1787. <https://doi.org/10.1016/j.biortech.2005.09.009>.
- [9] R. G. Saratale, G. D. Saratale, J. S. Chang, S. P. Govindwar, Decolorization and biodegradation of reactive dyes and dye wastewater by a developed bacterial consortium, *Biodegradation*, 21/6(2010) 999–1015. <https://doi.org/10.1007/s10532-010-9360-1>.
- [10] Y. Zhang, S. Zhang, J. Gao, and T.-S. Chung, Layer-by-layer construction of graphene oxide (GO) framework composite membranes for highly efficient heavy metal removal, *J. Memb. Sci.*, 515(2016) 230–237. <https://doi.org/10.1016/j.memsci.2016.05.035>.
- [11] D. K. Mahmoud, M. A. M. Salleh, W. A. W. A. Karim, A. Idris, Z. Z. Abidin, Batch adsorption of basic dye using acid treated kenaf fibre char: Equilibrium, kinetic and thermodynamic studies, *Chem. Eng. J.*, 181/182(2012). 449–457. <https://doi.org/10.1016/j.cej.2011.11.116>.
- [12] B. K. Körbahti, K. Artut, C. Geçgel, A. Özer, Electrochemical decolorization of textile dyes and removal of metal ions from textile dye and metal ion binary mixtures, *Chem. Eng. J.*, 173/3 (2011) 677–688. <https://doi.org/10.1016/j.cej.2011.02.018>.
- [13] P. Raizada, A. Sudhaik, P. Singh, Photocatalytic water decontamination using graphene and ZnO coupled photocatalysts: A review, *Mater. Sci. Energy Technol.*, 23/(2019) 509–525. <https://doi.org/10.1016/j.mset.2019.04.007>.
- [14] R. Naseem, S. S. Tahir, Removal of Pb(II) from aqueous/acidic solutions by using bentonite as an adsorbent, *Water Res.*, 35/16(2001). 3982–3986. [https://doi.org/10.1016/S0043-1354\(01\)00130-0](https://doi.org/10.1016/S0043-1354(01)00130-0).
- [15] M. El Ouardi, S. Qourzal, A. Assabbane, J. Douch, Adsorption studies of cationic and anionic dyes on synthetic ball clay, *Journal of Applied Surfaces and Interfaces.*, 1(1-3) (2017) 28-34
- [16] K. C. Lakshmi, N. Rao, K. Krishnaiah, Ashutos, Colour removal from a dyestuff industry effluent using activated carbon, *Indian journal of Chemical Ttechnology.*, 1(1994) 13-19.

- [17] I. D. Mall, V. C. Srivastava, N. K. Agarwal, I. M. Mishra, Removal of congo red from aqueous solution by bagasse fly ash and activated carbon: Kinetic study and equilibrium isotherm analyses, *Chemosphere*, vol. 61/ 4(2005) 492–501. <https://doi.org/10.1016/j.chemosphere.2005.03.065>.
- [18] I. D. Mall, V. C. Srivastava, N. K. Agarwal, I. M. Mishra, Adsorptive removal of malachite green dye from aqueous solution by bagasse fly ash and activated carbon-kinetic study and equilibrium isotherm analyses, *Colloids Surfaces A Physicochem. Eng. Asp.*, 264/1(2005)17–2. <https://doi.org/10.1016/j.colsurfa.2005.03.027>.
- [19] A. Talidi, M. Bouachrine, Etude de l'élimination du bleu de Méthylène en milieux aqueux par adsorption sur la pyrophyllite, *Revue Interdisciplinaire.*, 1/1(2016).
- [20] M. Abdallah, A. Hijazi, M. Hamieh, M. Alameh, Étude de l'adsorption du Bleu de Méthylène sur un biomatériau à base de l'eucalyptus selon la taille des particules Treatment of industrial wastewater using a natural and biodegradable adsorbent based on Eucalyptus, *Journal of materials and Environmental Science.*, 6/2(2016) 397–406..
- [21] F. Sakr, A. Sennaoui, M. Elouardi, M. Tamimi, A. Assabbane, Étude de l'adsorption du Bleu de Méthylène sur un biomatériau à base de Cactus (Adsorption study of Methylene Blue on biomaterial using cactus), *Journal of materials and Environmental Science.*, 6/ 2(2015). 397–406.
- [22] O. Khelifi, I. Mehrez, W. Ben Salah, F. Ben Salah, M. Younsi, M. Nacef, A.M. Affoune, Etude de l'adsorption du bleu de methylene (bm) a partir des solutions aqueuses sur un biosorbant prepare a partir des noyaux de datte algerienne, *Larhyss Journal.*, 28 (2016), 135-148.
- [23] M. T. Hadjyoussef, M. Jendoubi, M. Ben Amor, Removal of Fluoride from drinking water by an activated Bentonite: application to a drinking Tunisian, *Moroccan Journal of Chemistry.*, 6/1(2018) 6-1. <https://doi.org/10.48317/IMIST.PRSM/morjchem-v6i1.7772>.
- [24] A. Safae, N. Bennani, Z. Hamid, Q. Omar, Removing polyphenols contained in olive mill wastewater by membrane based on natural clay and Hydrotalcite Mg-Al, *Moroccan Journal of Chemistry.*, 8/1(2020) 318–325. <https://doi.org/10.48317/IMIST.PRSM/morjchem-v8i1.19171>.
- [25] B. Armağan, O. Özdemir, M. Turan, M. S. Celik, The removal of reactive azo dyes by natural and modified zeolites, *J. Chem. Technol. Biotechnol. Int. Res. Process. Environ. Clean Technol.*, 78/ 7(2003) 725–732. <https://doi.org/10.1002/jctb.844>.
- [26] E. Alver and A. Ü. Metin, Anionic dye removal from aqueous solutions using modified zeolite: Adsorption kinetics and isotherm studies, *Chem. Eng. J.*, 200/202(2012) 59–67. <https://doi.org/10.1016/j.cej.2012.06.038>.
- [27] C. Zannagui, H. Amhamdia, S. El Barkanyb, I. Jilalb, O. Sundmanc, A. Salhia, S. Chaoufa, M. Abou-Salamab, A. El Idrissid, M. Zaghrioui, Characterization and Investigation of Heavy Metal Ions Removal by New Cellulose-Ether Based adsorbent, *Moroccan Journal of Chemistry*, 8/ 1 (2020) 8-1.
- [28] L. Ouaya, A. H. Amoumi, Etude morphostructurale de la région de Nador (Maroc nord-oriental), *Africa Géosciences Review.*, 17/2(2010) 107–127.
- [29] D. M. Moore, R. C. Reynolds Jr, *X-ray Diffraction and the Identification and Analysis of Clay Minerals*. Oxford University Press (OUP)., (1989).
- [30] R. Khatem, ÉTUDE DES PROPRIÉTÉS ADSORBANTES DES ARGILES MODIFIÉES VIS-à-VIS DE POLLUANTS ORGANIQUES. CAS DE PRODUITS PHARMACEUTIQUE ET DES PESTICIDES. PhD Thesis, Université de Mostaganem-Abdelhamid Ibn Badis (2016).
- [31] L. Casagrande, Structures produced in clays by electric potentials and their relation to natural structures, *Nature*, 160/4066(1947) 470–471.
- [32] F. A. Andrade, H. A. Al-Qureshi, and D. Hotza, “Measuring the plasticity of clays: A review,” *Appl. Clay Mor. J. Chem.* 9 N°3 (2021) 416-433

Sci., 51/1 (2011) 1–7. <https://doi.org/10.1016/j.clay.2010.10.028>.

[33] T. N. Lan, Un Nouvel Essai d'Identification des Sols-L'Essai au Bleu de Méthylène, *Bull liaison lab ponts chauss.*, 88(1977).

[34] A. Medjnoun, R. Bahar, M. Khiatine, Caractérisation et estimation du gonflement des argiles algériennes, cas des argiles de Médéa, *MATEC Web of Conferences*, 11(2014) 3004.

[35] H. Ait Hmeid, M. Akodad, M. Aalaoul, M. Baghour, A. Moumen, A. Skalli, A. Anjjar, P. Conti, A. Sfalanga, F. Ryazi Khyabani, S. Minucci, L. Daoudi, Clay mineralogy, chemical and geotechnical characterization of bentonite from Beni Bou Ifrou Massif (The Eastern Rif-Morocco), *Geol. Soc. London, Spec. Publ.*, 502(2020) <https://doi.org/10.1144/SP502-2019-25>.

[36] A. Qlihaa, S. Dhimni, F. Melrhaka, N. Hajjaji, A. Srhiri, Caractérisation physico- chimique d ' une argile Marocaine, Physico-chemical characterization of a morrocan clay , *J. Mater. Environ. Sci.*, 7/5(2016) 1741-1750.

[37] I. Langmuir, The constitution and fundamental properties of solids and liquids. Part I. Solids., *J. Am. Chem. Soc.*, 38/11(1916) 2221–2295.

[38] W. J. Weber, J. C. Morris, Kinetics of adsorption on carbon from solution, *J. Sanit. Eng. Div.*, 89/2(1963) 31–60.

[39] H. Freundlich, Über die adsorption in lösungen, *Zeitschrift für Phys. Chemie*, 57/1(1907) 385–470.

[40] M. Peng, A. V Nguyen, J. Wang, and R. Miller, A critical review of the model fitting quality and parameter stability of equilibrium adsorption models, *Adv. Colloid Interface Sci.*, 262(2018) 50–68. <https://doi.org/10.1016/j.cis.2018.10.001>

[41] H. AitHmeid, M.Akodad, M.Aalaoul, M.Baghour, A. Moumen, A.Skalli, L.Daoudi., Particle size distribution and statistic analysis of the grain size messinian bentonite from the kert bassin (northern Morocco), *Mater. Today Proc.*, 13(2019) 505–514. <https://doi.org/10.1016/j.matpr.2019.04.007>.

[42] H. AitHmeid, M.Akodad, M.Aalaoul, M.Baghour, A. Moumen, A.Skalli, L.Daoudi, Characterization and Valuation of Clays in the North Eastern Region, *Euro-Mediterranean Conference for Environmental Integration* (2017) 1169-1172. https://doi.org/10.1007/978-3-319-70548-4_338

[43] H. AIT Hmeid, M. Akodad, M. Aalaoul, M. Baghour, A. Skalli, and L. Daoudi, petrographic , mineralogical and geochemical characterization of volcanic products from North-East Morocco, *International Journal of Development Research.*, 10/8(2020) 38714–38722. <https://doi.org/10.37118/ijdr.19364.08.2020>.

[44] Y. Millogo, Etude géotechnique, chimique et minéralogique de matières premières argileuse et latéritique du Burkina Faso améliorées aux liants hydrauliques: application au génie civil (bâtiment et route), *Univ. d'Ouagadougou, Th. Doct. Chim. minérale.*, (2008).

[45] S. D. J. Inglethorpe, D. J. Morgan, D. E. Highley, A. . Bloodworth, British Geological Survey: Industrial Minerals Laboratory Manual, *J. Math.*, (1993) 124.

[46] M. E. L. Alouani, S. Alehyen, M. E. L. Achouri, M. Taibi, Elaboration of Inorganic Polymer for Removal of Organic Compound by Dynamic Column Test, *Moroccan Journal of Chemistry.*, 7/1(2019) 10–16. <https://doi.org/10.48317/IMIST.PRSM/morjchem-v7i1.13890>

[47] S. Kumpulainen, L. Kiviranta, Mineralogical and Chemical Characterization of Various Bentonite and Smectite-Rich Clay Materials: Part A: Comparison and Development of Mineralogical Characterization Methods Part B: Mineralogical and Chemical Characterization of Clay Materials, *POSIVA Work. Rep.*, 52 (2010).

[48] P. S. Nayak, B. K. Singh, Instrumental characterization of clay by XRF, XRD and FTIR, *Bull. Mater. Sci.*, 30/3(2007) 235–238. <https://doi.org/10.1007/s12034-007-0042-5>.

[49] T. Ravindra Reddy, S. Kaneko, T. Endo, S. Lakshmi Reddy, Spectroscopic Characterization of Bentonite, *Mor. J. Chem.* 9 N°3 (2021) 416-433

- [50] H. Zaitan, D. Bianchi, O. Achak, and T. Chafik, "A comparative study of the adsorption and desorption of o-xylene onto bentonite clay and alumina," *J. Hazard. Mater.*, 153/1–2(2008) 852–859. doi:10.1016/j.jhazmat.2007.09.070.
- [51] M. Hajjaji, S. Kacim, M. Boulmane, Mineralogy and firing characteristics of a clay from the valley of Ourika (Morocco), *Appl. Clay Sci.*, 21/ 3–4 (2002) 203–212. [https://doi.org/10.1016/S0169-1317\(01\)00101-6](https://doi.org/10.1016/S0169-1317(01)00101-6).
- [52] W. Huang, J. Chen, F. He, J. Tang, D. Li, Y. Zhu, Y. Zhang, Effective phosphate adsorption by Zr/Al-pillared montmorillonite: insight into equilibrium, kinetics and thermodynamics. *Applied Clay Science*, 104(2015). 252-260. <https://doi.org/10.1016/j.clay.2014.12.002>.
- [53] Y. Bulut, Z. Tez, Removal of heavy metals from aqueous solution by sawdust adsorption, *J. Environ. Sci.*, vol. 19/2(2007) 160–166. [https://doi.org/10.1016/S1001-0742\(07\)60026-6](https://doi.org/10.1016/S1001-0742(07)60026-6).
- [54] K. M. S. Surchi, Agricultural Wastes as Low Cost Adsorbents for Pb Removal : Kinetics , Equilibrium and Thermodynamics, *International journal of chemistry.*, 3/3(2011) 103–112. doi:10.5539/ijc.v3n3p103.
- [55] O. Khelifi, I. Mehrez, W. B. Salah, F. B. Salah, M. Younsi, M. Nacef, A. Affoune, study of methylene blue (mb) adsorption from aqueous solutions on biosorbent prepared from algerian datte stones, *LARHYSS J.*, 28(2016), 135-148.
- [56] M. E. Argun, Use of clinoptilolite for the removal of nickel ions from water: Kinetics and thermodynamics, *J. Hazard. Mater.*, 150/3(2008) 587–595. <https://doi.org/10.1016/j.jhazmat.2007.05.008>.
- [57] S. Boumchita, A. Lahrichi, Y. Benjelloun, S. Lairini, V. Nenov, F. Zerrouq, Elimination d ' un colorant cationique dans une solution aqueuse par un déchet alimentaire : Epluchure de pomme de terre [Removal of cationic dye from aqueous solution by a food waste : Potato peel , *J. Mater. Environ. Sci.*, 7/1(2016) 73–84.
- [58] K. M. Kifuni, A. K. K. Mayeko, P. N. Vesituluta, B. I. Lopaka, G. E. Bakambo, B. M. Mavinga, J. M. Lunguya, Adsorption d ' un colorant basique , Bleu de Méthylène , en solution aqueuse , sur un bioadsorbant issu de déchets agricoles de Cucumeropsis mannii Naudin Adsorption of basic dye , Methylene Blue , in aqueous solution on bioadsorbent from agricultural waste of Cucumeropsis Naudin mannii, *International Journal of Biological and Chemical Sciences.*, 12/1(2018) 558–575. DOI: 10.4314/ijbcs.v12i1.43.
- [59] J. Reungoat, J.-S. Pic, M.-H. Manero, H. Debellefontaine, Adsorption of nitrobenzene from water onto high silica zeolites and regeneration by ozone, *Sep. Sci. Technol.*, 42/7(2007) 1447–1463. <https://doi.org/10.1080/01496390701289948>.
- [60] A. Reffas, V. Bernardet, B. David, L. Reinert, M. Bencheikh Lehocine, M. Dubois, N. Batisse, L. Duclaux, Carbons prepared from coffee grounds by H₃PO₄ activation: Characterization and adsorption of methylene blue and Nylosan Red N-2RBL, *J. Hazard. Mater.*, 175/1(2010) 779–788. <https://doi.org/10.1016/j.jhazmat.2009.10.076>
- [61] S. S. Tahir, N. Rauf, Removal of a cationic dye from aqueous solutions by adsorption onto bentonite clay, *Chemosphere*, 63/11(2006) 1842–1848. <https://doi.org/10.1016/j.chemosphere.2005.10.033>.
- [62] N. Cherfaoui, R. Djebri, Etude de l'adsorption du colorant (bleu de méthylène) sur un charbon actif préparé à partir des noyaux du Genévrier oxycédre. *PhD thesis, Université de Bouira*, (2017).
- [63] K. Khaldi, M. Hadjel, A. Benyoucef, Removal of quinmerac by diatomite and modified diatomite from aqueous solution, *Surf. Eng. Appl. Electrochem.*, 54/2(2018) 194–202. <https://doi.org/10.3103/S1068375518020084>.
- [64] O. Hamdaoui, M. Chiha, Removal of Methylene Blue from Aqueous Solutions by Wheat Bran., *Acta Chim. Slov.*, 54/2(2007).
- [65] Y. Miyah, M. Idrissi, A. Lahrichi, F. Zerrouq, Removal of a Cationic Dye–Méthylène Bleu–From Aqueous Solution by Adsorption onto Oil Shale Ash of Timahdit (Morocco), *International Journal of Innovative Research in Mor. J. Chem.* 9 N°3 (2021) 416-433

Science, Engineering and Technology, 3/8(2014).

[66] K. Boudouara, M. Ghelamallah, and K. Benzaoui, Kinetic and equilibrium studies of methyl violet adsorption from aqueous solutions by activated Algerian bentonite clay, *Arab. J. Geosci.*, 12/15(2019) 459. <https://doi.org/10.1007/s12517-019-4626-3>.